

Preparation and mechanical properties of aluminum alloy 5a02/cfrtp laminates

Jiuming Xie¹, Cong She², Jiang Sun³, Xuejun Zhou¹, Jie Ding¹

¹Tianjin Sino-German University of Applied Science, School of Mechanical Engineering, No. 2, Yashen Road, Jinnan District, 300000, Tianjin, China.

²Tianjin University of Technology, No. 391, Binshui West Road, Xiqing District, 300000, Tianjin, China.

³Tianjin Renai College, Tuanbo New City, Jinghai District, 300000, Tianjin, China.

e-mail: xiejiuming1983@163.com, 13752119958@163.com, sam_renai@163.com, zhouxuejun1978@163.com, dingjie@tsguas.edn.cn

ABSTRACT

Aerospace and military defense fields are posing higher requirement on the lightweight feature of structures. Subject of this study is the Aluminum Alloy 5A02 /CFRTP (Carbon Fiber Reinforced Thermo-Plastic) laminates. In the paper, aluminum alloy was anodized, compression molding and 3D printing were adopted to prepare Carbon Reinforced Aluminum Laminates (CARALL) with two different structures: the solid core structure and the honeycomb structure, and the prepared specimens were then tested for mechanical properties via tensile test and three-point bending test, and compared with the performance of the conventional aluminum alloy. The results show that under the condition of a same thickness, the tensile strength of CARALL specimens with the molded solid core structure and the 3D printed honeycomb structure reaches 256Mpa and 186MPa, respectively, which is 85.5% and 34.8% higher than that of the tensile strength of Al 5A02; under different bending modes, the maximum bending strength is 682Mpa and 525Mpa, respectively, which is 62.4% and 25.5% higher than that of Al 5A02. When the specimens are subject to tensile force, the separation of the metal layer and the fiber layer is the primary failure form, the fiber layer fractures, and the metal layer exhibits the necking phenomenon as the metal fibers are being pulled out. During the bending process, for different bending forms, there're great differences in the bending strength of CARALL specimens prepared by the same method, the failure modes of the specimens vary greatly as well, and this is determined by the tensile strength of the carbon fiber layer and the tensile strength of AL 5A02. Enhancing the bonding strength between the metal layer and the fiber layer can improve the mechanical properties of CARALL. These research findings can provide a reference for the lightweight design of metals and Fiber Metal Laminates (FMLs).

Keywords: lightweight; CARALL (Carbon Reinforced Aluminum Laminates); compression molding, 3D printing; honeycomb structure.

1. INTRODUCTION

The rapid advance of military defense, aerospace, rail transit, and navigation fields puts higher demands on the properties of components and requires them to develop towards to the directions of high performance, light-weight, precise, reliable, and economical [1–3]. To answer to these requirements, it's urgent for researchers to develop materials with higher strength, lower density, and higher damage tolerance. Fiber Metal Laminates (FMLs) perfectly integrate the good properties of both the conventional fiber composite materials and the metal materials by overlaying the light metal and the reinforced composite material layer by layer, and it has become one of the most popular lightweight materials in various fields [4, 5]. Especially in the aerospace industry, about 470 m² of the wall plates on the upper part of the fuselage of Airbus A380 uses FMLs, which reduces the total weight of the aircraft by nearly one ton. FMLs is also adopted in structures such as the aircraft skin, the flat tail and the vertical tail front edge [6].

As early as in 1970, the Dutch company Fokker began to experiment on fiber-reinforced resin and metal composites [7]. In 1980, the FMLs developed by the Delft University of Technology has attracted wide attention from field scholars, and this has been regarded as the symbol of the birth of FMLs [8]. After that, world field scholars have conducted a lot of research on the design, development, preparation, mechanical properties, and damage of FML, the number of varieties of FMLs increases greatly, examples of FMLs include

the titanium-based FMLs, aluminum-based FMLs, magnesium-based FMLs and stainless steel-based FMLs. Carbon Reinforced Aluminum Laminates (CARALL) are aluminum laminates reinforced by carbon fibers developed in recent years, and they are also called the third-generation FMLs. They have the merits of high elastic modulus, low density, good damage tolerance, and excellent mechanical properties. Different preparation methods, component materials and fiber layer sequences can produce FMLs with different properties and functions. REYES V. and CANTWELL [9] prepared CFRP (carbon fiber reinforced polymer) laminates through molding and analyzed the tensile performance, fatigue performance and stamping performance of the laminates. BIENIAŚ and JAKUBCZAK [10] prepared Al/CFRP/AL laminates using an autoclave method and studied the influence of different laying directions of carbon fibers on the mechanical properties of the laminates. WANG *et al.* [11] used rolling process to prepare Al/CFRP/AL laminates and studied their molding properties. KHALILI *et al.* [12] and CORTÉS and CANTWELL [13] prepared aluminum-based FMLs by means of hot pressing and studied their fracture toughness and tensile performance. ZAFAR *et al.* [14] prepared FMLs using a method based on simultaneous forming of any number of multiple metallic blanks in re-quired shape by applying hydroforming technology, their study provides an effective method and direction for the fabrication of FMLs components. WEI *et al.* [15] added a flexible layer composed of polyether tri-amine between CFRP and aluminum foil, after subjected to low temperature cycles, the interface bonding performance of the aluminum foil/CFRP laminates has been improved significantly.

The latest advancement of aerospace and military defense fields has imposed a series of high standards and demands for the equipment container boxes of electronic devices, requiring them to be mini-sized, lightweight, and integrated. The equipment container boxes of electronic devices need a large number of screws, during their service life, they need to bear loads and thermal shocks, and shield the electronic devices contained in them. The original equipment boxes made of aluminum alloy can no longer meet the increasingly demanding lightweight requirement, so it's necessary to develop the AB-type FMLs to lighten the weight of the aluminum alloy equipment boxes. Taking the load and thermal shock requirements under actual working conditions into consideration, this paper used PEEK-based compo-sites reinforced by carbon fibers and the aluminum alloy 5A02 material to design and fabricate AB-type CARALL flat plate structure via compression molding and 3D printing, tested its tensile and bending performance and compared with the aluminum alloy flat plate. The research of this paper could serve as a reference for the lightweight design of electronic device containers, and it has certain theoretical and practical values.

2. MODELING

2.1. Raw materials

The aluminum alloy material used in the experiment is aluminum alloy 5A02, which is commonly used in the aerospace field, the thickness of the material is 1 mm and is provided by Highsort Advanced Materials (Tianjin) Co., Ltd. The chemical composition of the material is shown in Table 1.

The CARALL specimens prepared by compression molding adopted the belt prepreg of PEEK-based composite material reinforced by carbon fibers, the model is EW300 and is also provided by Highsort Advanced Materials (Tianjin) Co., Ltd., the specific feature parameters are shown in Table 2.

The CARALL specimens prepared by 3D printing adopted the PEEK-based composite material reinforced by carbon fibers, the model is Kexcelled peek K10CF and is provided by North Bridge New Material Technology (Suzhou) Co., Ltd., the specific feature parameters are shown in Table 3.

Names and sources of specimen preparation equipment are shown in Table 4.

Table 1: Chemical composition of aluminum alloy 5A02.

ELEMENT	MASS FRACTION (%)
Si	0.20
Fe	0.30
Cu	0.10
Mn	0.25
Mg	2.2
Ti	0.15
Al	Remain
Others	<0.15

Table 2: Feature parameters of prepreg.

INDICATOR	VALUE
Weaving form	Plain weave
Width (mm)	500 mm × 500 mm
Surface density of fabric(g/m ²)	300 ± 15
Resin content (%)	50 ± 10
Thickness of prepreg (mm)	0.35–0.50

Table 3: Feature parameters of prepreg.

INDICATOR	VALUE
Wire diameter (mm)	1.75 ± 0.03 mm
Density (g/cm ³)	1.15
Resin content (%)	10 ± 0.5

Table 4: Sample preparation equipment.

EQUIPMENT NAME	BRAND	MODEL	REMARK
Flexible integrated technology platform	Tianjin Sino-German University of Applied Sciences	Self-built	Automatic molding equipment
3D printer	WIIBOOX	WIIBOOX D600PRO	
Water-jet cutter	Shenyang HEAD Science Technology Co. Ltd.	HEAD 20	Cutting machine of specimen

2.2. Preparation of materials

The interface properties of aluminum alloy 5A02 and carbon fiber composites have obvious effects on the tensile and bending performance and failure mode of the structure of composites. In order to ensure the inter-layer bonding performance of aluminum alloy and carbon fiber composites, it's necessary to perform surface treatment on the aluminum alloy, and the commonly used surface treatment methods of aluminum alloy include the mechanical treatment, chemical treatment, and electrochemical treatment. Previous research showed that anodizing can form nanoscale to macroscopic structures on the surface of aluminum alloy [16–18], which can effectively improve the bonding strength of aluminum alloy and carbon fiber reinforced composites.

In this study, anodizing was adopted to perform surface treatment on the aluminum alloy, and the processing flow is shown in the figure 1 below.

Liquid components and processing parameters of anodizing bath are shown in Table 5 below.

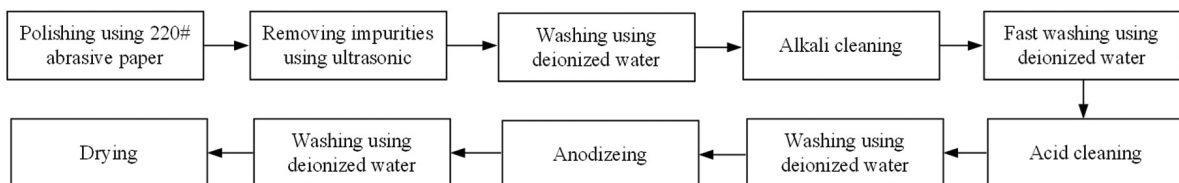


Figure 1: Processing flow of anodizing.

Table 5: Liquid components and processing parameters of anodizing bath.

BATH LIQUID COMPONENTS	PARAMETER
Phosphoric acid (HPO ₄)	100 g/L
Low voltage at bath end	30 V
Stirring speed of bath liquid	200 r/min
Temperature	25 ± 2°C
Anodizing time (t)	15 min

Compression molding was adopted to prepare the CARALL specimens, size of the prepreg is 500 mm × 500 mm. During the experiment, release agent was brushed on the mold; to prevent resin spill of prepreg during the molding process, a doughnut-shaped frame was set on the mold. The system adopted oil heating and cooling, and the processing flow of compression molding is shown in Figure 2.

During the process of compression molding, the closed mold was placed on a pressing table, the unit pressure was maintained at about 0.8 MPa during the heating process. When the temperature of the top and bottom of the mold reached 370–380°C, the pressure was increased to 1.5–2.0MPa and kept for 20 min, after that, the pressure was unloaded and the temperature was cooled down at a speed of 5°C/min. When the temperature declined to 60°C, the mold was opened, the processing flow is shown in Figure 3.

The CARALL specimens prepared by compression molding were cut as shown in Figure 4.

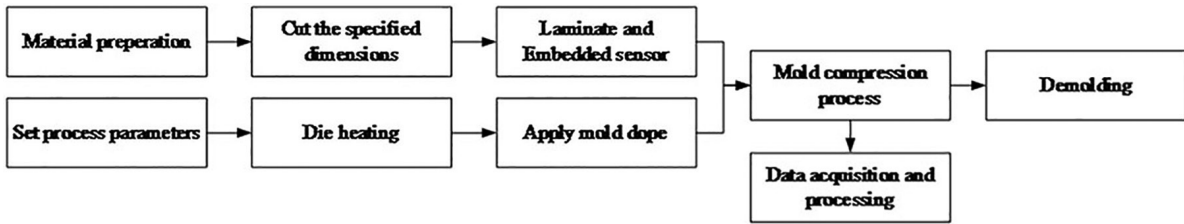


Figure 2: Experimental process of compression molding.

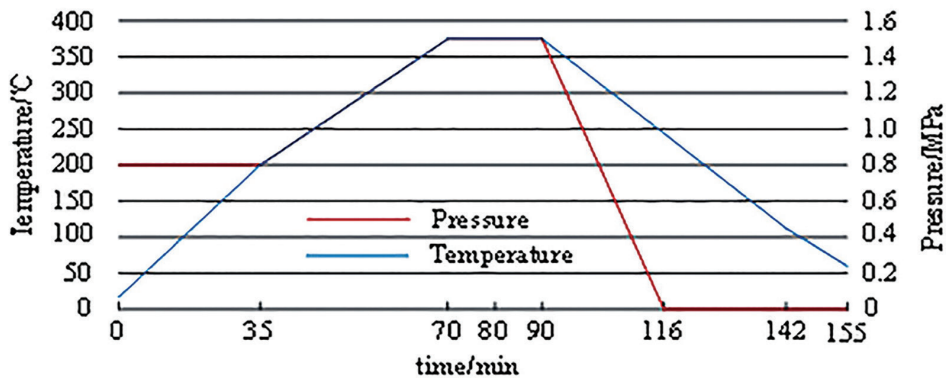


Figure 3: Curing process of CFTRP.

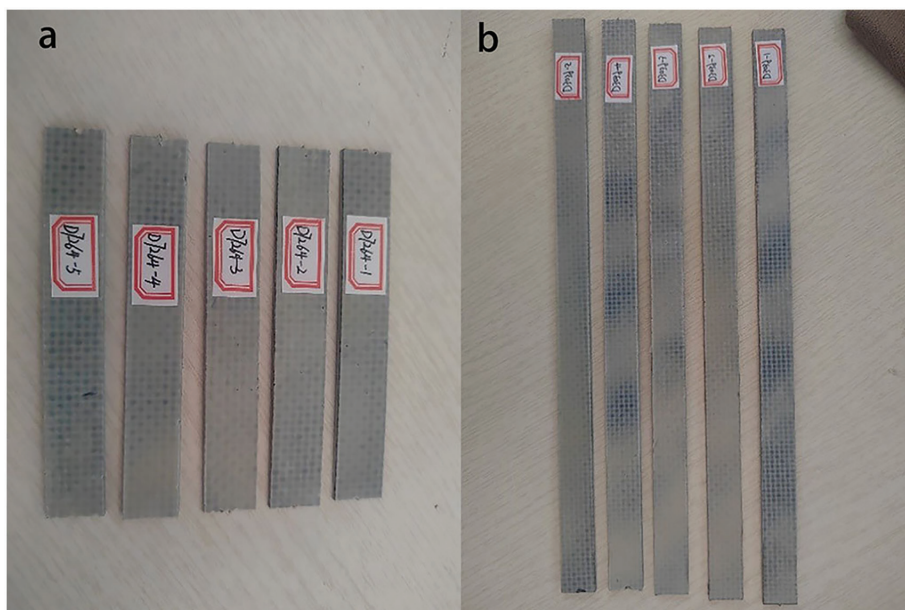


Figure 4: CARALL specimens prepared by compression molding: (a) Specimens for tensile test; (b) Specimens for three-point bending test.

Table 6: Processing parameters of 3D printed CARALL specimens.

PRINTING PROCESS	PARAMETER
Printing temperature	420 ± 5°C
Preheating temperature of aluminum alloy	120 ± 5°C
Cavity temperature	110 ± 10°C
Printing speed	35 ± 2 mm/s

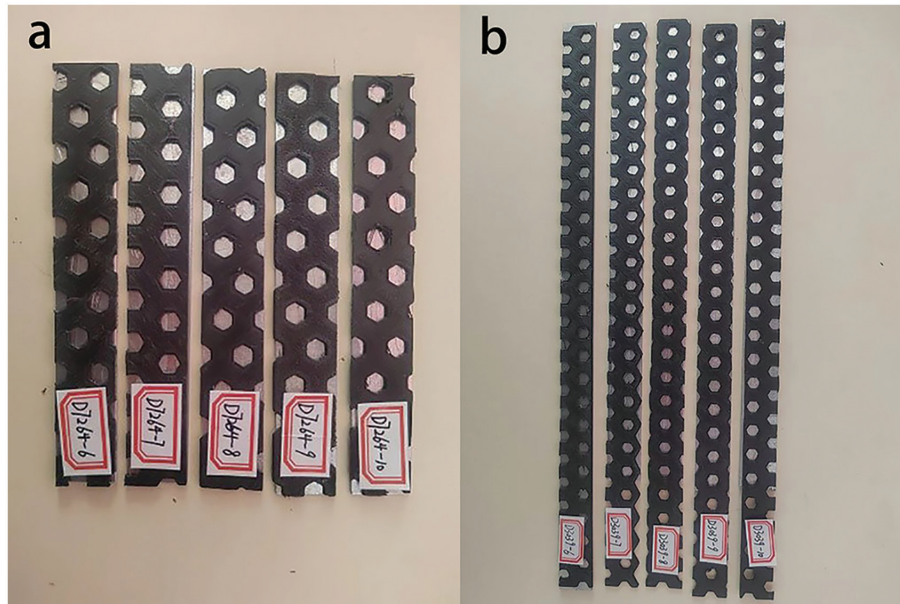


Figure 5: CARALL specimens prepared by 3D printing: (a) Specimens for tensile test; (b) Specimens for three-point bending test.

When using 3D printing to prepare composites in the carbon fiber layer of the CARALL specimens, the adopted processing parameters are shown in Table 6.

To better achieve the lightweight requirement, based on the good mechanical properties of honeycomb structure [19, 20], the carbon fiber layer was designed as the honeycomb structure. The CARALL specimens prepared by 3D printing are shown in Figure 5.

2.3. Testing and characterization

To measure the mechanical properties of CARALL specimens prepared through different methods, their physical properties, tensile performance and bending performance were tested.

The thickness of the aluminum alloy plates and the CARALL specimens was measured using a digital vernier caliper, and it's ensured that the thickness of the laminates processed by the two processing techniques was consistent, and the accuracy of the digital vernier caliper is 0.01 mm.

After the aluminum alloy was anodized, thin tubular holes that are uniformly distributed, regular shaped, and nearly perpendicular to the surface of the aluminum alloy were formed on the aluminum alloy surface. The size and depth of the holes, and the number of holes on per unit area of the surface will affect the interlayer bonding performance of the CARALL specimens. Porosity is the ratio of the total volume of the holes to the total volume of the oxide film layer. Then, the surface observer SEM was used for observation and the porosity was calculated.

According to the ASTM D3039-Standard Test Method for Tensile Properties of Polymer Matrix Composite Materials [21], the tensile performance of CARALL was tested on a universal testing machine, and the loading rate was 2 mm/min.

According to the ASTM D7264-Standard Test Method for Flexural Properties of Polymer Matrix Composite Materials [22], the CARALL specimens were subject to three-point bending test on the universal test machine, the pre-pressure was 5N, and the loading rate was 1 mm/min.

3. RESULTS AND DISCUSSION

3.1. Test on physical properties of CARALL

The thickness of CARALL specimens prepared by the two methods was tested, as shown in Figure 6.

According to Figure 6, the thickness of CARALL specimens prepared by the two methods was the same. For the CARALL specimens prepared by compression molding, under the action of pressure during the molding process, the overall thickness of the CARALL after molding was slightly less than the laying thickness before molding. For the CARALL specimens prepared by 3D printing, through the compensation of printing thickness, the consistency of the thickness of CARALL specimens was ensured.

3.2. Interface microstructure of CARALL

Figure 7 gives SEM photos of anodized film formed on the surface of aluminum alloy after subjected to acid and alkali corrosion and polished by the 220 # abrasive paper. In low-power SEM photo, it can be seen that the anodized film of the aluminum alloy shows a bumped appearance similar to the crystal cell structure of metals, this is because during the anodizing process, the phosphoric acid did not destroy the original appearance of the aluminum alloy surface after subjected to the acid and alkali corrosion. In high-power SEM photo, it's found that on the aluminum alloy surface, a porous nano-structured oxide film had been formed, the pores distributed uniformly and the arrangement was regular.

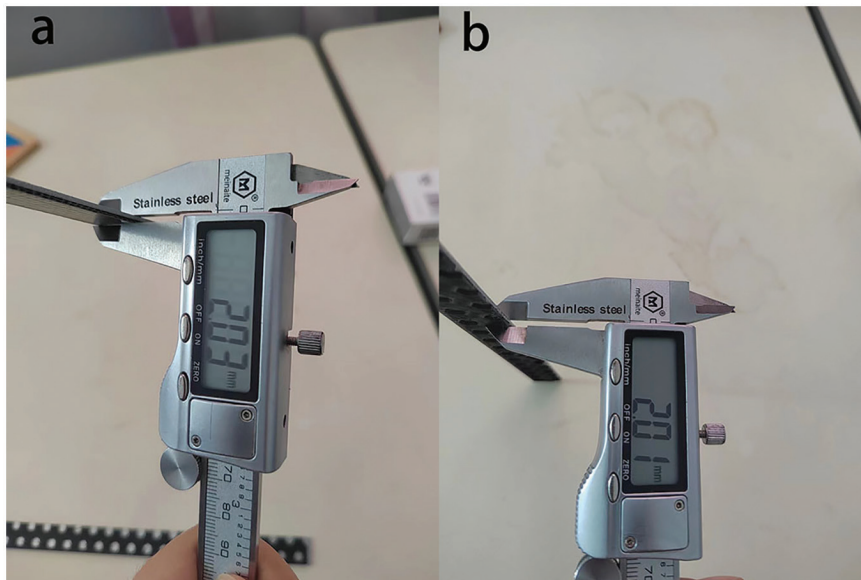


Figure 6: Thickness test of CARALL: (a) Specimens prepared by compression molding; (b) Specimens prepared by 3D printing.

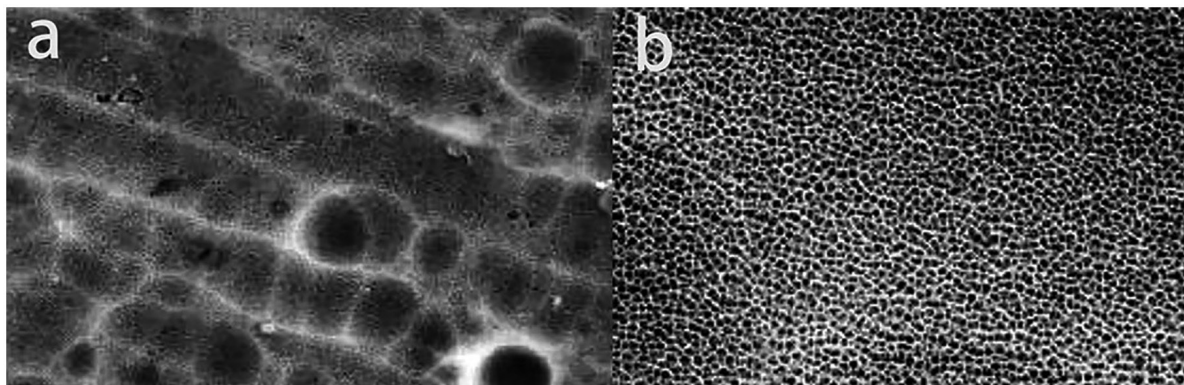


Figure 7: SEM photos of anodized aluminum alloy surface: (a) Low-power SEM Photo; (b) High-power SEM Photo.

3.3. Test on tensile performance of CARALL

The process of the CARALL tensile performance test is shown in Figure 8. For each group of specimens, the test was performed for five times, and the test results were averaged.

Tensile test was carried on the CARALL specimens prepared by the two methods, all of them showed obvious separation and fracture of the metal layer and the fiber layer, and the separation behavior was prior to the fracture, exhibiting as the primary failure form of CARALL. Figure 9 shows the macroscopic structure of CARALL after the tensile test, it can be seen from the figure that for the CARALL specimens prepared by the two methods, during the tensile process, the aluminum alloy layer shows obvious necking and fracture behaviors. For CARALL specimens prepared by compression molding, the fibers in the carbon fiber layer were pulled out from the matrix and fractured, during the experimental process, the carbon fiber layer exhibited failure prior to the aluminum alloy layer. In the 3D printing process of CARALL, the carbon fiber layer showed the fracture behavior of honeycomb structure. Similarly, the fiber layer showed the failure behavior before the aluminum alloy layer during the experiment.

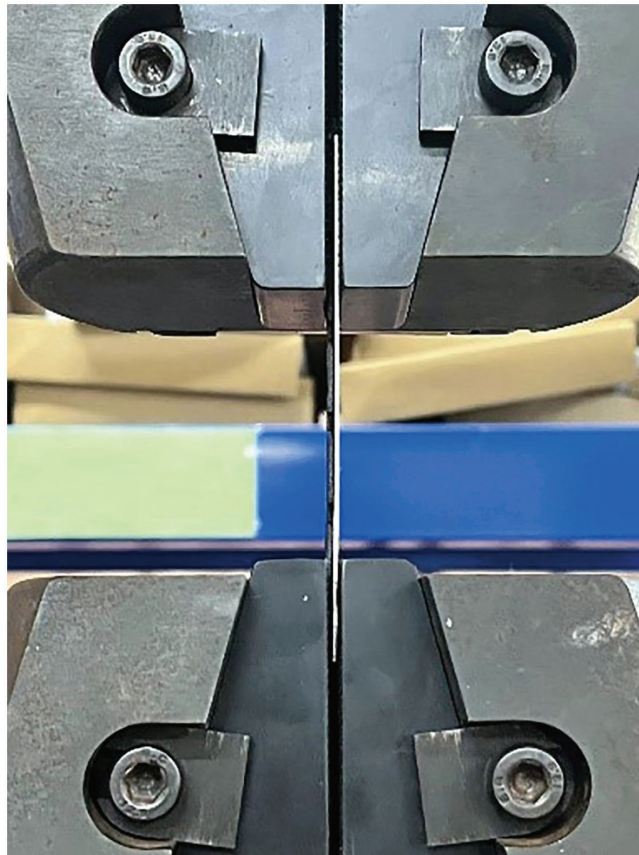


Figure 8: Process of the tensile test.

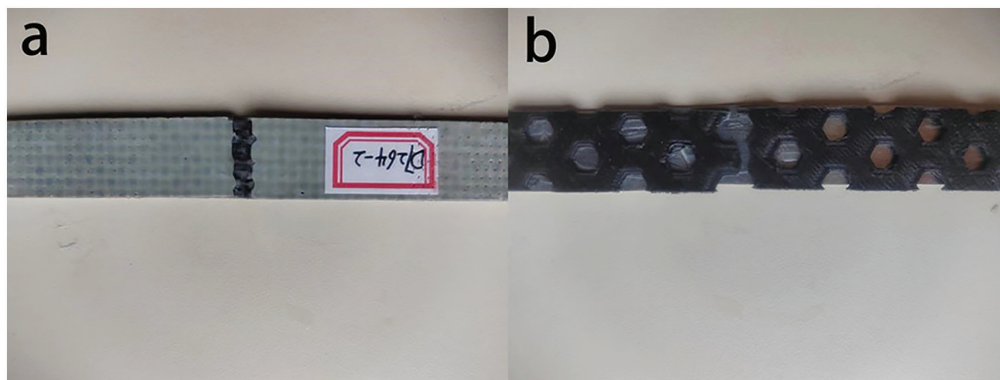


Figure 9: Macrostructure after tensile test: (a) Molding process specimen; (b) 3D printing process specimen.

Tensile test was performed on CARALL specimens with a plate thickness of 2 mm prepared by the two methods. Under the condition of a same thickness, the tensile strength of CARALL specimens prepared by compression molding reached 256MPa and the tensile strength of CARALL specimens prepared by 3D printing reached 186Mpa, which were respectively 85.5% and 34.8% higher than the tensile strength of Al 5A02. The ten-sile strength of CARALL prepared by 3D printing was lower. On the one hand, the 3D printed honeycomb structure had greatly reduced the cross-sectional area of the fiber layer; on the other hand, under the action of the tensile force, stress was concentrated at the sharp corners on each edge of the honeycomb structure.

3.4. Test on bending performance of CARALL

Figure 10 shows the process of the three-point bending test of CARALL. For the AB-type CARALL specimens, three-point bending test was performed on the A-side and B-side (namely the fiber layer and the metal layer) of the specimens from different directions, as shown in the two photos of Figure 10.

During the test on the three-point bending performance of CARALL prepared by two methods, the specimens all showed obvious separation of the metal layer and the fiber layer. Figure 11 shows the macrostructure of the different surfaces of molded CARALL after the three-point bending test, wherein photos (a) and (b) are the three-point bending test on the metal layer, and photos (c) and (d) are the three-point bending test on the fiber layer. As can be seen in (a) and (b), at the bending positions, the separation of fiber layer and metal layer is not obvious, but on the edge of the bending parts, the separation appears, and the fiber layer shows obvious cracks, which is the fracture between the matrix. As can be seen in (c) and (d), the fiber layer and metal layer show obvious separation, there's no obvious crack, and the metal layer exhibits slight necking phenomenon.

Figure 12 shows the macrostructure of 3D printed CARALL with a honeycomb structure after the three-point bending test. Photos (a) and (b) are the three-point bending test on the metal layer, and photos (c) and (d) are the three-point bending test on the fiber layer. As can be seen in (a) and (b), the fiber layer shows fractures and it separates obviously from the metal layer at the bending part, the metal layer shows obviously necks and cracks. During the test, the fracture of fiber layer is prior to the separation, which is the main failure form of the three-point bending of CARALL. In (c) and (d), the fiber layer and the metal layer show obvious separation, three groups show fiber layer fractures, and the metal layer of all groups shows obvious necks and slight cracks. It is considered that for the 3D printed CARALL with a honeycomb structure, during the three-point bending test, the fracture of the fiber layer and the necking and cracking of the metal layer happen at the same time, and it's the main failure form.

CARALL specimens with a plate thickness of 2 mm prepared by the two methods were subjected to the three-point bending test. Under the condition of a same thickness, the bending strength of CARALL prepared by compression molding reached 682MPa and 616MP respectively. This is because during the three-point bending, the carbon fibers were subjected to the action of tensile force, and it had a higher strength. The aluminum alloy layer was under the action of compression and had a better toughness, therefore, its bending strength was high-er. The bending strength of the 3D printed honeycomb-structured CARALL reached 465MPa and 525MPa re-spectively, this is because the tensile performance of the honeycomb structure is lower, which has resulted in that the bending strength under tensile state is smaller. For the CARALL prepared by the two methods, the maximum bending strength is 62.4% and 25.5% higher than the bending strength of Al 5A02, respectively.

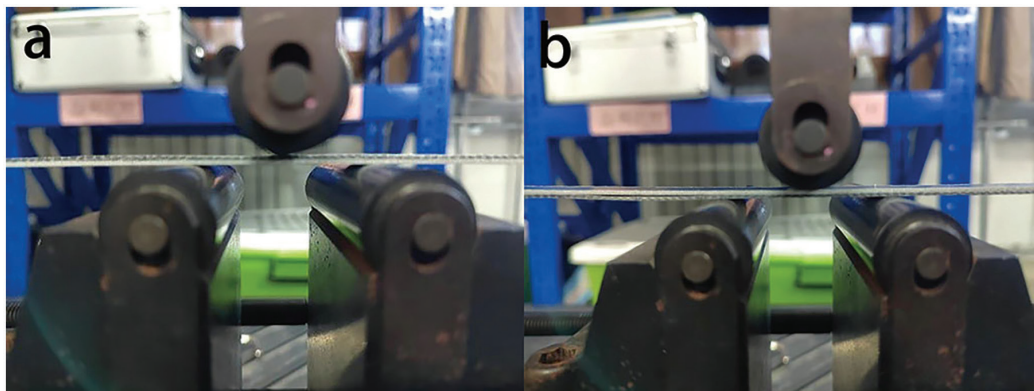


Figure 10: Process of the three-point bending test: (a) Fibre layer on top; (b) Metal layer on top.

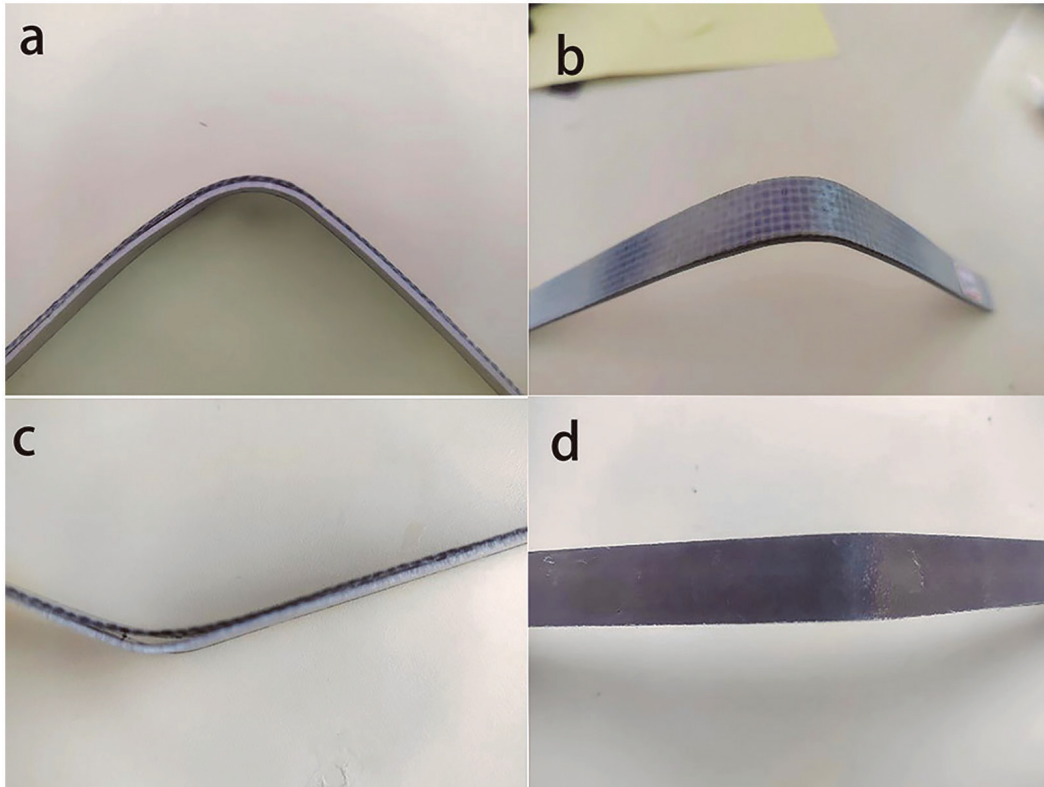


Figure 11: Macrostructure of molded CARALL after the three-point bending test: (a) The metal layer is layered on top; (b) Cracks when metal layer is on top; (c) The fiber layer is layered on top; (d) Necking when fiber layer on top.

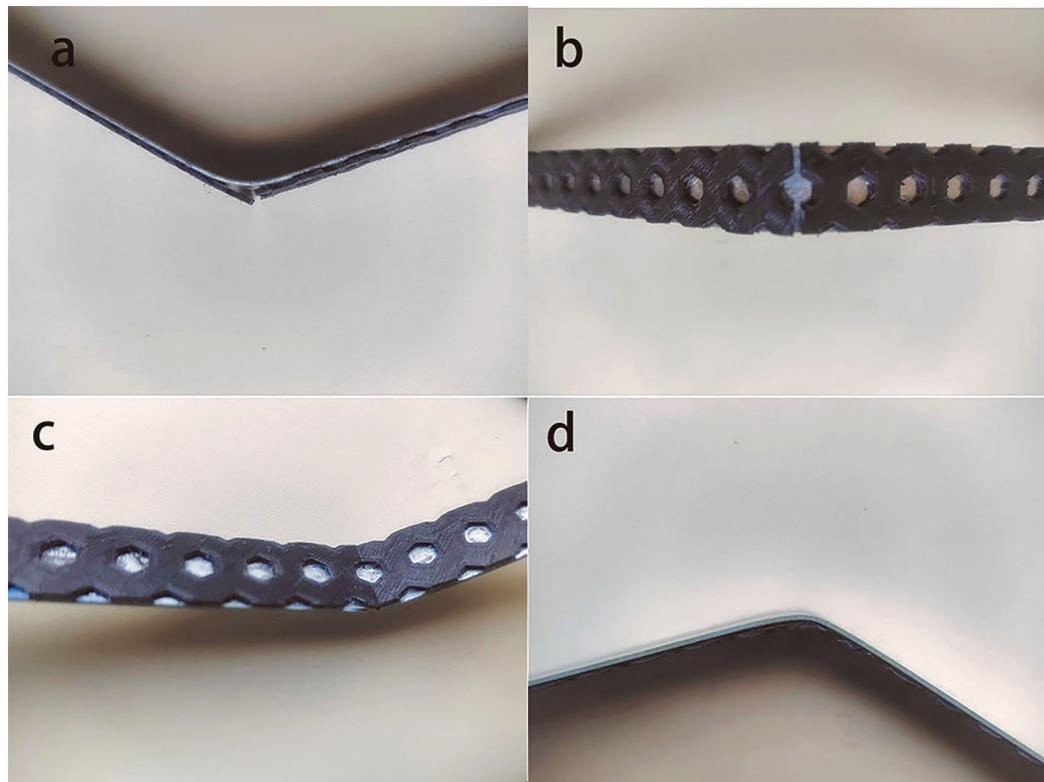


Figure 12: Macrostructure of 3D printed CARALL with a honeycomb structure after the three-point bending test: (a) The metal layer is layered on top; (b) The metal layer breaks when it is up; (c) The fiber layer breaks when it is up; (d) The fiber layer is layered on top.

4. CONCLUSIONS

To respond to the lightweight requirement of aerospace and military defense fields, this paper adopted compression molding and 3D printing to design CARALL specimens with two types of structures: the solid core structure and the honeycomb structure. Then, the paper tested their tensile performance and bending performance, and analyzed their failure forms and principles. After the metal surface was anodized, thin tubular holes formed and distributed on the metal surface, which can enhance the bonding effect between the carbon fiber layer and the metal layer. The results of tensile test of CARALL showed that, under a same thickness, the tensile strength of CARALL prepared by compression molding can reach 256MPa, and the tensile strength of 3D printed CARALL with a honeycomb structure can reach 186MPa, which is 85.5% and 34.8% higher than the tensile strength of Al 5A02, respectively. The results of three-point bending test of CARALL showed that, under a same thickness, the bending strength of CARALL prepared by compression molding can reach 682MPa, and the tensile strength of 3D printed CARALL with a honeycomb structure can reach 525MPa, which is 62.4% and 25.5% higher than the tensile strength of Al 5A02, respectively. In the three-point bending test, under different bending modes, there're great differences in the bending strength of CARALL specimens prepared by the same method, and there're large differences in their failure form as well, this is mainly determined by the tensile strength of the carbon fiber layer and the tensile strength of AL 5A02. Research results showed that, during the stretching and bending process of CARALL, the separation of fiber layer and metal layer is obvious, by effectively enhancing the bonding strength between the layers, the tensile and bending performance of CARALL can be improved to a certain extent.

5. BIBLIOGRAPHY

- [1] ZHAN, S., ZHANG, P., "Key Basic Scientific Issues for Near Space Vehicles major research program concluded", *China Science Foundation*, v. 1, pp. 6, 2017.
- [2] DU, S., "Advanced composites and aerospace", *Journal of Composite Materials*, v. 24, pp. 12, 2007.
- [3] PRAVEEN KUMAR, A., DIRGANTARA, T., VAMSI KRISHNA, P., *Advances in lightweight materials and structures*, USA, Springer, 2020.
- [4] LEE, M.S., SEO, H.Y., KANG, C.G., "Comparison of collision test results for center-pillar reinforcements with TWB and CR420/CFRP hybrid composite materials using experimental and theoretical methods", *Composite Structures*, v. 168, pp. 698–709, 2017. <http://dx.doi.org/10.1016/j.compstruct.2017.02.068>.
- [5] PRAMANIK, A., BASAK, A.K., DONG, Y., *et al.*, "Joining of carbon fiber reinforced polymer (CFRP) composites and aluminium alloys-A review", *Composites. Part A, Applied Science and Manufacturing*, v. 101, pp. 1–29, 2017. <http://dx.doi.org/10.1016/j.compositesa.2017.06.007>.
- [6] FRIZZELL, R.M., MCCARTHY, C.T., MCCARTHY, M.A., "An experimental investigation into the progression of damage in pin-loaded fibre metal laminates", *Composites. Part B, Engineering*, v. 39, n. 6, pp. 907–925, 2008. <http://dx.doi.org/10.1016/j.compositesb.2008.01.007>.
- [7] VLOT, A., VOGELANG, L.B., VRIES, T., "Towards application of fibre metal laminates in large aircraft", *Aircraft Engineering*, v. 72, pp. 558–570, 2000.
- [8] AGHAMOHAMMADI, H., HOSSEINI ABBANDANAK, S.N., ESLAMI-FARSANI, R., *et al.*, "Effects of various aluminum surface treatments on the basalt fibre metal laminates interlaminar adhesion", *International Journal of Adhesion and Adhesives*, v. 84, pp. 184–193, 2018. <http://dx.doi.org/10.1016/j.ijadhadh.2018.03.005>.
- [9] REYES, V., G., CANTWELL, W.J., "The mechanical properties of fibre-metal laminates based on glass fibre reinforced polypropylene", *Composites Science & Technology*, v. 60, n. 7, pp. 1085–1094, 2000. [https://doi.org/10.1016/S0266-3538\(00\)00002-6](https://doi.org/10.1016/S0266-3538(00)00002-6).
- [10] BIENIAŚ, J., JAKUBCZAK, P., "Low velocity impact resistance of aluminium/carbon-epoxy fiber metal laminates", *Composite Theory and Practice*, v. 3, pp. 193–197, 2012.
- [11] WANG, J., ZHANG, L., QIN, H., "Carbon fiber/epoxy composite laminates prepared by rolling and their forming properties", *Journal of Composites Science*, v. 35, pp. 2601–2611, 2018.
- [12] KHALILI, S.M.R., MITTAL, R.K., KALIBAR, S.G., "A study of the mechanical properties of steel/aluminium/GRP laminates", *Materials Science and Engineering A*, v. 412, n. 1–2, pp. 137–140, 2005. <http://dx.doi.org/10.1016/j.msea.2005.08.016>.
- [13] CORTÉS, P., CANTWELL, W., "Fracture properties of a fiber-metal laminates based on magnesium alloy", *Journal of Materials Science*, v. 39, n. 3, pp. 1081–1083, 2004. <http://dx.doi.org/10.1023/B:JMSE.0000012949.94672.77>.

- [14] ZAFAR, R., LANG, L., ZHANG, R., “Experimental and numerical evaluation of multilayer sheet forming process parameters for light weight structures using innovative methodology”, *International Journal of Material Forming*, v. 9, n. 1, pp. 35–47, 2016. <http://dx.doi.org/10.1007/s12289-014-1198-3>.
- [15] WEI, R., WANG, X.Q., CHEN, C., *et al.*, “Effect of surface treatment on the interfacial adhesion performance of aluminum foil/CFRP laminates for cryogenic propellant tanks”, *Materials & Design*, v. 116, pp. 188–198, 2017. <http://dx.doi.org/10.1016/j.matdes.2016.12.011>.
- [16] PAULOSE, M., PRAKASAM, H.E., VARGHESE, O.K., *et al.*, “TiO₂ nanotube arrays of 1000 Mu M length by anodization of titanium foil: phenol red diffusion”, *The Journal of Physical Chemistry C*, v. 111, n. 41, pp. 14992–14997, 2007. <http://dx.doi.org/10.1021/jp075258r>.
- [17] ZHANG, J., ZHAO, X., ZUO, Y., *et al.*, “The bonding strength and corrosion resistance of aluminum alloy by anodizing treatment in a phosphoric acid modified boric acid/sulfuric acid bath”, *Surface and Coatings Technology*, v. 202, n. 14, pp. 3149–3156, 2008. <http://dx.doi.org/10.1016/j.surfcoat.2007.10.041>.
- [18] BJØRGUM, A., LAPIQUE, F., WALMSLEY, J., *et al.*, “Anodising as pre-treatment for structural bonding”, *International Journal of Adhesion and Adhesives*, v. 23, n. 5, pp. 401–412, 2003. [http://dx.doi.org/10.1016/S0143-7496\(03\)00071-X](http://dx.doi.org/10.1016/S0143-7496(03)00071-X).
- [19] LYU, L., WANG, R., LIU, W., “Design, preparation and properties of wave absorbing composites with Beehive 3-D integral woven structure”, *Journal of Composite Materials*, v. 40, pp. 1–7, 2022.
- [20] LIU, X., WU, Q., YU, G., “Three-point bending properties of carbon fiber/resin-based composite beehive sandwich structures”, *Applied Mathematics and Mechanics*, v. 43, pp. 9, 2022.
- [21] AMERICAN SOCIETY FOR TESTING AND MATERIALS, *ASTM D3039 Standard Test Method for Tensile Properties of Polymer Matrix Composite Materials*, New Jersey, West Conshohocken, Wiley, 2008.
- [22] AMERICAN SOCIETY FOR TESTING AND MATERIALS, *ASTM D7264 Standard Test Method For Flexural Properties of Polymer Matrix Composite Materials*, New Jersey, West Conshohocken, Wiley, 2010.